Inhibition of Histone Deacetylase Activity Suppresses Epithelial-to-Mesenchymal Transition Induced by TGF-β1 in Human Renal Epithelial Cells

Masahiro Yoshikawa, Keiichi Hishikawa, Takeshi Marumo, and Toshiro Fujita

Department of Internal Medicine, Division of Nephrology and Endocrinology, and Department of Clinical Renal Regeneration, Graduate School of Medicine, University of Tokyo, Tokyo, Japan

Histone acetylation plays an important role in regulating gene expressions by modulating chromatin structure. Histone deacetylase (HDAC) inhibitors have been reported to have an antifibrogenic effect in some organs, such as the liver, skin, and lung, but the underlying mechanisms remain to be clarified. In the kidney, bone morphologic protein 7 (BMP-7) and hepatocyte growth factor are reported to antagonize TGF-β1–induced tubular epithelial-to-mesenchymal transition (EMT), but nothing is known concerning the effect of HDAC inhibitors on EMT. It was shown that trichostatin A (TSA), an HDAC inhibitor, prevented TGF-β1–induced EMT in cultured human renal proximal tubular epithelial cells. Treatment with TGF-β1 induced morphologic changes such as EMT in human renal proximal tubular epithelial cells. However, co-treatment with TSA completely prevented TGF-β1–induced morphologic changes and significantly prevented TGF-β1–induced downregulation of E-cadherin and upregulation of collagen type I. Treatment with TSA did not alter TGF-β1–induced phosphorylation of Smad2 and Smad3 but induced several inhibitory factors of TGF-β1 signals, such as inhibitors of DNA binding/differentiation 2 (Id2) and BMP-7. Chromatin immunoprecipitation assay confirmed that histone acetylation was involved in the downregulation of E-cadherin and upregulation of Id2 and BMP-7. These results suggest that TSA and other HDAC inhibitors could be new therapeutic agents for tubular EMT.

J Am Soc Nephrol 18: 58–65, 2007. doi: 10.1681/ASN.2005111187

Tubulointerstitial fibrosis in the kidney is one of the common and representative findings of many chronic renal diseases. In progressive states, it causes irreversible renal dysfunction, necessitating renal replacement therapy (1,2). Many factors have been reported to be fibrogenic in the kidney. Particularly, TGF-β1 induces tubular epithelial-to-mesenchymal transition (EMT) (3,4) and is thought to be one of the major causes of renal fibrosis. It is thought that TGF-β1 plays a significant role in the progression of diabetic nephropathy (5) and also in an experimental rodent model of unilateral urinary obstruction (1).

All members of the TGF-β superfamily transmit their signals through type I and type II serine/threonine kinase receptors (2). Upon TGF-β1 stimulation, the type II receptor phosphorylates the type I receptor, which subsequently phosphorylates receptor-regulated Smad proteins (R-Smads) Smad2 and/or Smad3. Then phosphorylated R-Smads form heterocomplexes with common Smad protein Smad4 and translocate into the nucleus and regulate the transcription of TGF-β1 target genes (2,6–8). It is reported that besides Smad signaling, TGF-β1 signals can be transmitted *via* other signal transduction pathways in human kidney cells, such as p38 mitogen-activated protein kinase, Akt/protein kinase B, and RhoA (7,9). However, TGF-β1–induced tubular EMT seems to depend primarily on Smad signaling (7).

Many kinds of therapeutics to reverse TGF-β1–induced tubular EMT have been investigated. Bone morphologic proteins (BMP) are members of the TGF-β superfamily, whose signals are transmitted *via* phosphorylated Smad1, Smad5, and Smad8 (2). In this pathway, BMP-7 signals directly antagonize TGF-β1 signals at the transcription level and reverse TGF-β1–induced tubular EMT (3). Another renotrophic factor, hepatocyte growth factor (HGF), is reported to block TGF-β1–induced EMT (10,11). It is suggested that HGF antagonizes TGF-β1 signals by inducing Smad transcriptional co-repressors such as Ski-related novel gene (SnoN) and TG-interacting factor (TGIF) (10), but the underlying mechanisms remain largely unknown (12). Recently, it was reported that some epithelial cells that overexpress inhibitors of DNA binding/differentiation (Id) ectopically showed resistance to TGF-β1–induced EMT (13,14), but its exact mechanisms also still are unclear.

Histone acetylation is mediated by mutually opposing activities of histone acetyltransferases (HAT) and histone deacetylases (HDAC) (15,16). When HAT are activated or HDAC are suppressed, more histones are acetylated and the chromatin structure becomes relaxed, then transcriptional regulators are able to access promoter regions of genes more easily and modify their expression positively or negatively (15). HAT and HDAC activities are altered in several cancer cells (17), and

Received November 15, 2005. Accepted October 5, 2006.

Published online ahead of print. Publication date available at www.jasn.org.

Address correspondence to: Dr. Keiichi Hishikawa, Department of Internal Medicine, Division of Nephrology and Endocrinology, The University Hospital of Tokyo, Hongo 7-3-1, Bunkyo-ku, Tokyo 113-8655, Japan. Phone: +81-3-3815-5411 ext. 35725; Fax: +81-3-5800-9738; E-mail: hishikawa-tky@umin.ac.jp

ISSN: 1046-6673/1801-0058

HDAC inhibitors now are promising anticancer agents whose effects are correlated with the transcriptional regulation of specific cancer-related genes (17,18). HDAC inhibitors also are shown to have an antifibrogenic effect. Tricostatin A (TSA), an HDAC inhibitor, inhibited transdifferentiation of hepatic stellate cells into myofibroblasts (19) and also abrogated TGF-β1–inducing fibrosis-related gene expression in skin fibroblasts (15). In human pulmonary fibrosis, phenylbutyrate, a weaker HDAC inhibitor, decreased collagen type I production (20). However, it still largely is unknown how these HDAC inhibitors act against fibrosis. In this study, we investigated whether TGF-β1–induced tubular EMT can be suppressed by TSA in human renal proximal tubular epithelial cells (RPTEC) and attempted to reveal its underlying mechanisms.

Materials and Methods

Cell Culture and Treatment

Human RPTEC and culture medium (REGM BulletKit) that contained 0.5% FBS, hydrocortisone (0.5 μg/ml), EGF (10 ng/ml), epinephrine (0.5 μg/ml), triiodothyronine (6.5 ng/ml), transferrin (10 μg/ml), insulin (5 μg/ml), gentamicin (50 μg/ml), and amphotericin (50 ng/ml) were purchased from Cambrex Corp. (East Rutherford, NJ). RPTEC (three to five passages) were cultured in REGM BulletKit on culture plates to subconfluence and then treated with 3 ng/ml TGF-β1 (R&D Systems, Minneapolis, MN) and/or TSA (Biomol Research Laboratories, Plymouth Meeting, PA) at the indicated concentrations for the indicated periods of time.

Real-Time Reverse Transcriptase–PCR

Total RNA was extracted with an RNeasy Mini Kit (Qiagen K.K., Tokyo, Japan) following the manufacturer's protocol. cDNA was synthesized from total RNA samples by reverse transcription with high-capacity cDNA archive kit (Applied Biosystems, Foster City, CA) following the manufacturer's protocol. Quantitative real-time reverse transcriptase–PCR was performed using commercially available TaqMan probes (E-cadherin, Hs00170423_m1; collagen type I, Hs00164004_m1; BMP-7, Hs00233476_m1; HGF, Hs00300159_m1; Ski, Hs00161707_m1; SnoN, Hs00180524_m1; TGIF, Hs00820148_g1; Id1, Hs00357821_g1; Id2, Hs00747379_m1; Id3, Hs00171409_m1; and glyceraldehyde-3-phosphate dehydrogenase, 4326317E) and analyzed on an ABI PRISM 7000 sequence detector system (Applied Biosystems). Quantitative values were obtained from the threshold PCR cycle number at which an increase in signal that was associated with exponential growth of the PCR product started to be detected. The relative mRNA levels in each sample were normalized to its glyceraldehyde-3-phosphate dehydrogenase content.

Western Immunoblot Analysis

RPTEC were lysed in sample buffer that contained 50 mM Tris-HCl (pH 6.8), 2% SDS, 6% β-mercaptoethanol, and 10% glycerol. After homogenization of samples on ice, total protein concentration was measured with an RC DC protein assay kit (Bio-Rad, Hercules, CA) following the manufacturer's protocol. Equal amounts of total proteins were boiled and separated on SDS-polyacrylamide gels (Bio-Rad). Then the proteins were transferred onto a nitrocellulose membrane (Hybond-ECL; Amersham, Arlington Heights, IL) in transfer buffer that contained 25 mM Tris, 0.192 M glycine, and 20% methanol. The membrane was blocked for 1 h in 2% BSA dissolved in Tris-buffered saline (20 mM Tris, 0.8% NaCl, and 0.1% Tween20 [pH 7.6]) that contained 0.1% Tween20 (TBST) and then incubated for 1 h with primary antibodies to E-cadherin (BD Pharmingen, San Jose, CA), β-actin, Smad2/3 (Santa Cruz Biotechnology, Santa Cruz, CA), acetylated histones (Upstate Biotechnology, Lake Placid, NY), phospho-Smad2 (Cell Signaling Technology, Beverly, MA), or phospho-Smad3 (Novus Biologicals, Littleton, CO), followed by the respective horseradish peroxidase–linked secondary antibody (Amersham) diluted appropriately in TBST that contained 1% BSA. After washing with TBST, the immunoreactive proteins were detected by an enhanced chemiluminescence detection system (Amersham). The relative protein levels of E-cadherin and acetylated histones in each sample were normalized to its β-actin content, and the relative phosphorylation levels of Smad2 and Smad3 protein in each sample were normalized to its Smad2/3 protein content (21).

Immunofluorescence Staining of Collagen Type I

RPTEC that were plated on Lab-Tek chamber slides (Nalge Nunc International, Rochester, NY) were treated with 3 ng/ml TGF-β1 and/or 1000 nM TSA for 48 h. The cells were fixed with cold methanol and blocked in 2% goat serum diluted in PBS that contained 0.1%

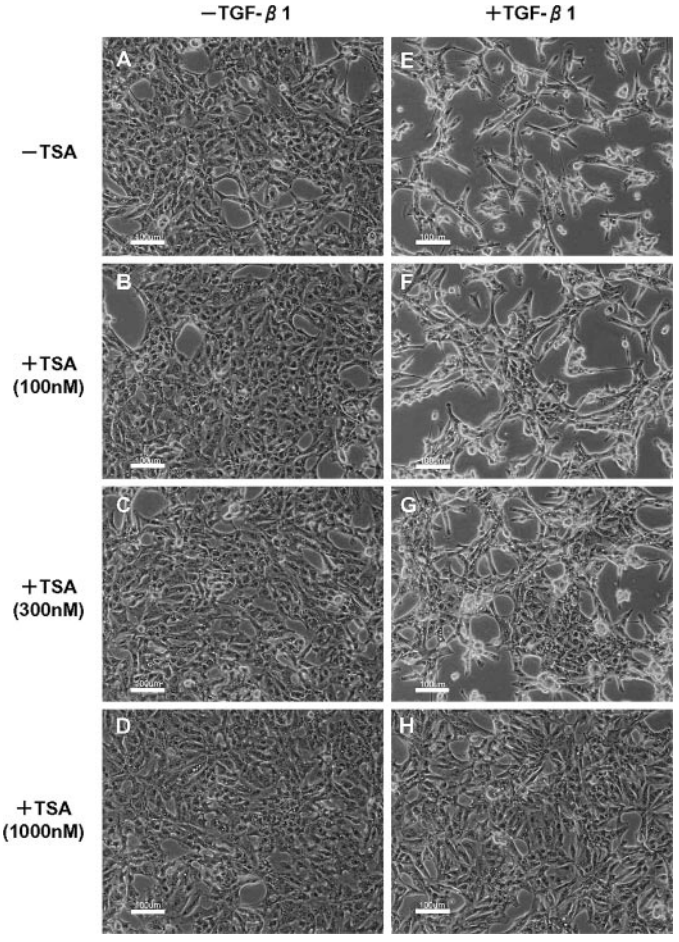

Figure 1. Trichostatin A (TSA) prevents TGF-β1–induced epithelial-to-mesenchymal transition (EMT)-like morphologic changes in human renal proximal tubular epithelial cells (RPTEC). RPTEC were treated with TSA in the presence and absence of TGF-β1 (3 ng/ml) for 24 h. Representative morphologic changes are shown. (A) Control RPTEC. (B) 100 nM TSA alone (C) 300 nM TSA alone. (D) 1000 nM TSA alone. (E) TGF-β1 alone (F) TGF-β1 and 100 nM TSA. (G) TGF-β1 and 300 nM TSA. (H) TGF-β1 and 1000 nM TSA. Bar = 100 μm.

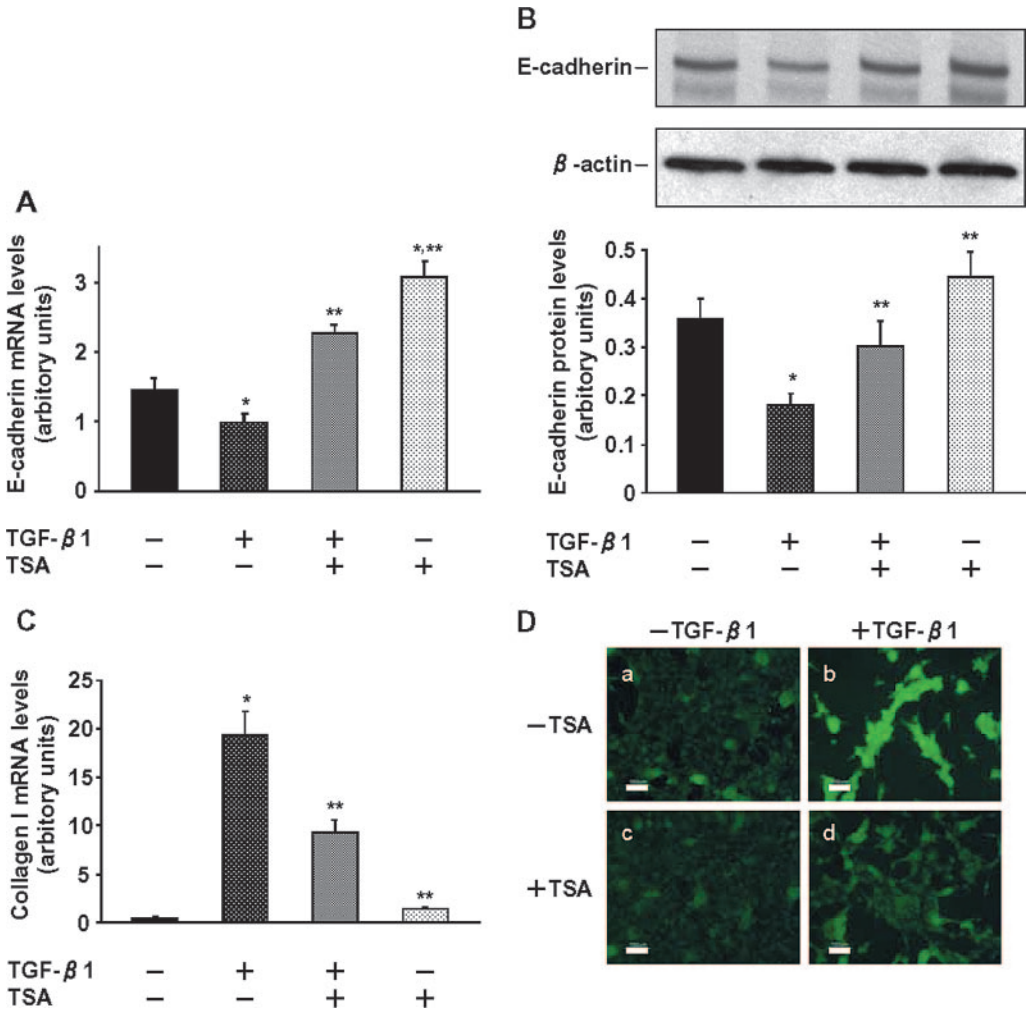

Figure 2. TSA prevents TGF-β1–induced downregulation of E-cadherin and upregulation of collagen type I in human RPTEC. (A through C) RPTEC were treated with TGF-β1 (3 ng/ml) and TSA (300 nM) for 24 (A and B) or 12 h (C). Data are means ± SEM of at least five independent experiments. *$P < 0.05$ *versus* control; **$P < 0.05$ *versus* TGF-β1–treated RPTEC. (A) Gene expression of E-cadherin was quantified by real-time reverse transcriptase–PCR (RT-PCR). (B) Representative Western immunoblot of E-cadherin protein (top) and its graphical presentation (bottom). (C) Gene expression of collagen type I was quantified by real-time RT-PCR. (D) RPTEC were treated with TGF-β1 (3 ng/ml) and TSA (1000 nM) for 48 h. Expression of collagen type I protein was examined by immunofluorescence with anti–collagen type I antibody. Data are representative of four independent experiments. Bar = 100 μm.

Tween20 and then incubated overnight with anti–collagen type I goat polyclonal antibody (Chemicon International, Temecula, CA) followed by Alexa Fluor 488 anti-goat antibody (Molecular Probes, Eugene, OR) diluted in blocking solution. After washing with PBS that contained 0.1% Tween20, the stained cells were mounted with Vecta Shield mounting medium (Vector Laboratories, Burlingame, CA) and viewed with an Eclipse TS100 microscope (Nikon, Tokyo, Japan).

Chromatin Immunoprecipitation Assay

Chromatin immunoprecipitation (ChIP) assay was performed with an Acetyl-Histone Immunoprecipitation Assay Kit (Upstate Biotechnology) following the manufacturer's protocol. Briefly, approximately 1×10^6 cells in a six-well culture plate were incubated with 1% formaldehyde diluted in culture medium for 10 min at 37°C. Each sample that was lysed in SDS lysis buffer (kit component) that contained protease inhibitors (1 mM PMSF, 1 μg/ml aprotinin, and 1 μg/ml pepstatin A) was sonicated on ice to shear DNA to lengths between 200 and 1000 bp and incubated with primary antibodies to acetylated histones overnight at 4°C on a shaker plate. Then samples were incubated with Salmon Sperm DNA/Protein A Agarose Slurry (kit component) for 1 h at 4°C on a shaker plate. After washing several times with washing buffers (kit components), the pelleted protein A agarose/antibody/histone complex was incubated with elution buffer (1% SDS and 0.1 M $NaHCO_3$) for 15 min at room temperature. Then the samples were incubated with 0.2 M NaCl for >4 h at 65°C. After DNA was recovered by phenol/chloroform extraction and ethanol precipitation, PCR was performed using the following primers: E-cadherin promoter (GenBank accession no. L34545), 5′-AGCCCCATCTCCAAAACGA-3′ and 5′-TTATGGGACCTGCACGGTTC-3′; Id2 promoter (22), 5′-GTTGCAAAAGCCCACACTAAGC-3′ and 5′-GTTCACTGCAACCCATCGG-3′; and BMP-7 promoter (GenBank accession no. AF210054), 5′-GCGGAGAAGATCGCTGATC-3′ and 5′-ATCAGACGCTGCTTTCTCCT-3′. Aliquots of samples before immunoprecipitation (Input) also were analyzed by PCR to quantify the amount of DNA present in different

samples. The relative DNA levels in each sample were normalized to its Input DNA levels (23).

Statistical Analyses

All results are expressed as mean ± SEM. Paired *t* test and Fisher protected least significant difference test were used for statistical comparison. $P < 0.05$ was considered statistically significant.

Results

TSA Prevents TGF-β1–Induced EMT-Like Morphologic Changes in Human RPTEC

It is known that TGF-β1 induces EMT in many kinds of epithelial cells and changes their shape from a cuboidal to a more elongated form, a so-called spindle-like shape, *in vitro* (6,24–27). Cultured human RPTEC without treatment showed a cuboidal shape (Figure 1A), and treatment with TGF-β1 alone made their shape spindle-like (Figure 1E). Conversely, treatment with TSA in the presence of TGF-β1 prevented TGF-β1–induced morphologic changes in a concentration-dependent manner (Figure 1, F through H). Cells that were treated with TSA alone did not change morphologically (Figure 1, B through D).

TSA Prevents TGF-β1–Induced Downregulation of E-Cadherin and Upregulation of Collagen Type I in Human RPTEC

E-cadherin is expressed in epithelial cells and is regarded as a marker of epithelial cells (25). Treatment with TGF-β1 alone reduced gene expression of E-cadherin to approximately 70% of control (Figure 2A). However, co-treatment with TSA prevented the downregulation of E-cadherin almost completely (Figure 2A). To clarify the effect of TSA on the protein level of E-cadherin in human RPTEC, we performed Western blot. Treatment with TGF-β1 alone reduced protein expression of E-cadherin to approximately 50%, but co-treatment with TSA significantly prevented the reduction (Figure 2B). Next, we examined gene expression of collagen type I, which is regarded as a reliable marker of fibrosis in many organs (15,19,20,28). As shown in Figure 2C, treatment with TGF-β1 alone markedly increased gene expression of collagen type I by approximately 20-fold, but co-treatment with TSA reduced it almost to 50%. This also was the case for protein expression. Cells that were treated with TGF-β1 alone showed a strong signal of collagen type I, but co-treatment with TSA showed a faint signal (background level; Figure 2D). Because TSA alone increased E-cadherin and collagen I mRNA, these results suggest that TSA is not a specific antagonist for TGF-β1 but may antagonize indirectly TGF-β1–induced EMT by inducing several factors that counteract TGF-β1.

TSA Does Not Alter TGF-β1–Induced Phosphorylation of Smad2 and Smad3

TGF-β1 transmits its signals by binding to its type I and type II receptors, which subsequently phosphorylate receptor-regulated Smad proteins Smad2 and/or Smad3 (2,7). To clarify the mechanism of the inhibitory effect of TSA on TGF-β1 signals, we investigated the effect of TSA on TGF-β1–induced phosphorylation of Smad2 and Smad3. As shown in Figure 3, TGF-β1 alone induced phosphorylation of Smad2 and Smad3,

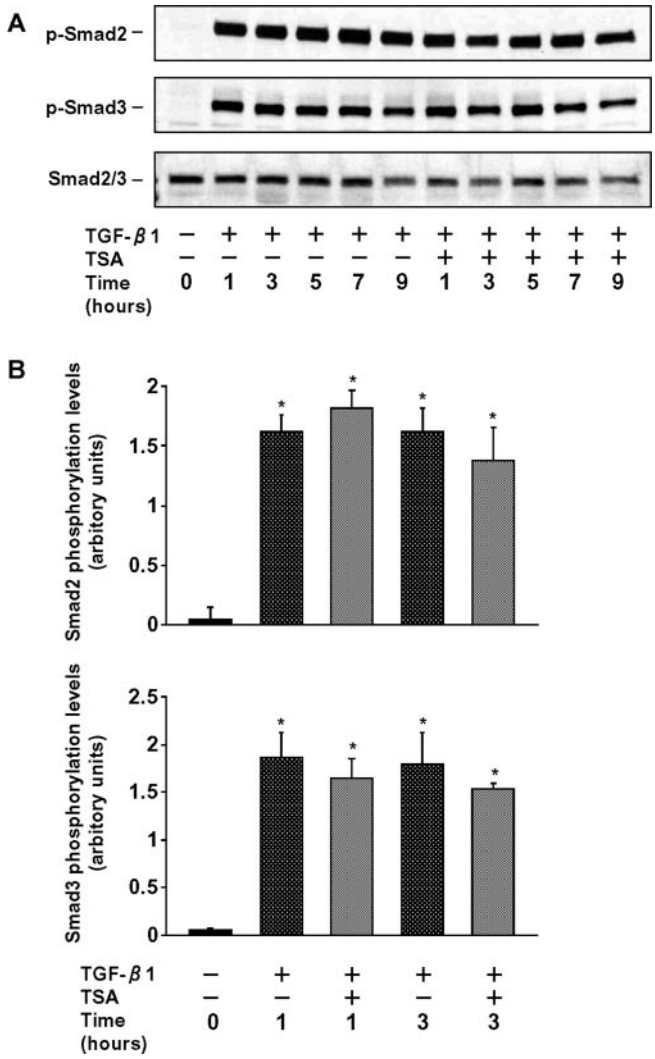

Figure 3. TSA does not alter TGF-β1–induced phosphorylation of Smad2 and Smad3. RPTEC were treated with TGF-β1 (3 ng/ml) and TSA (300 nM) for the indicated periods of time. Representative Western immunoblot of phosphorylated Smad2 (p-Smad2) and Smad3 (p-Smad3) (A) and its graphical presentation (B) are shown. Data are means ± SEM of five independent experiments. *$P < 0.05$ *versus* control.

but co-treatment with TSA showed no effect. These results suggest that TSA does not suppress TGF-β1 signals at the level of Smad2 and Smad3 phosphorylation but at a downstream level. Because TSA failed to affect Smad2 and Smad3 phosphorylation, we tried to examine the downstream pathways. We performed ChIP assay for the collagen type I gene by antibodies against phosphorylated Smad2 and Smad3, respectively, but the results were not clear (data not shown).

TSA Induces Several Inhibitory Factors of TGF-β1

Several factors have been reported to have an antifibrogenic effect or to antagonize TGF-β1 signals, such as BMP-7 (1–3); HGF (7,10); Ski, SnoN, and TGIF (5,10,29); and Id1, Id2, and Id3 (13,14). Therefore, we investigated whether TSA induces these factors by quantitative real-time PCR. Treatment with TGF-β1

alone showed no effect on gene expression of Id2 and BMP-7, but co-treatment with TSA significantly upregulated it (Figure 4). Treatment with TGF-β1 alone significantly upregulated gene expression of Id1 and SnoN, but co-treatment with TSA hardly upregulated it (data not shown). We also examined the gene expression of HGF, TGIF, Ski, and Id3, but treatment of TSA showed little effect (data not shown). To confirm the results of real-time PCR, we performed Western blot. However, we could not get significant changes, suggesting that real-time PCR may be more sensitive to detect changes of these factors in our model.

TSA-Induced Histone Remodeling Is Involved in Downregulation of E-Cadherin and Upregulation of Id2 and BMP-7

To investigate whether acetylated histones H3 and H4 were increased by treatment with TSA, we performed Western blot. As shown in Figure 5, the amount of acetylated histones H3 and H4 was significantly increased by treatment with TSA in the presence and absence of TGF-β1. We next performed ChIP assay for the E-cadherin, Id2, and BMP-7 genes. As compared with treatment with TGF-β1 alone, co-treatment with TSA significantly increased acetylated histones H3 and H4 in the E-cadherin promoter region: H3 in the Id2 promoter region and H4 in the BMP-7 promoter region (Figure 6).

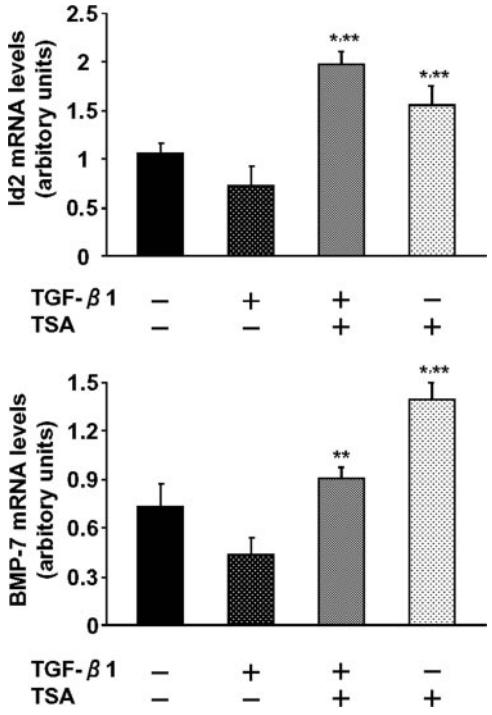

Figure 4. TSA induces several inhibitory factors of TGF-β1. RPTEC were treated with TGF-β1 (3 ng/ml) and TSA (300 nM) for 6 (inhibitors of DNA binding/differentiation 2 [Id2]) or 12 h (bone morphologic protein 7 [BMP-7]). Gene expression of Id2 and BMP-7 was quantified by real-time RT-PCR. Data are means ± SEM of at least six independent experiments. *$P < 0.05$ *versus* control; **$P < 0.05$ *versus* TGF-β1–treated RPTEC.

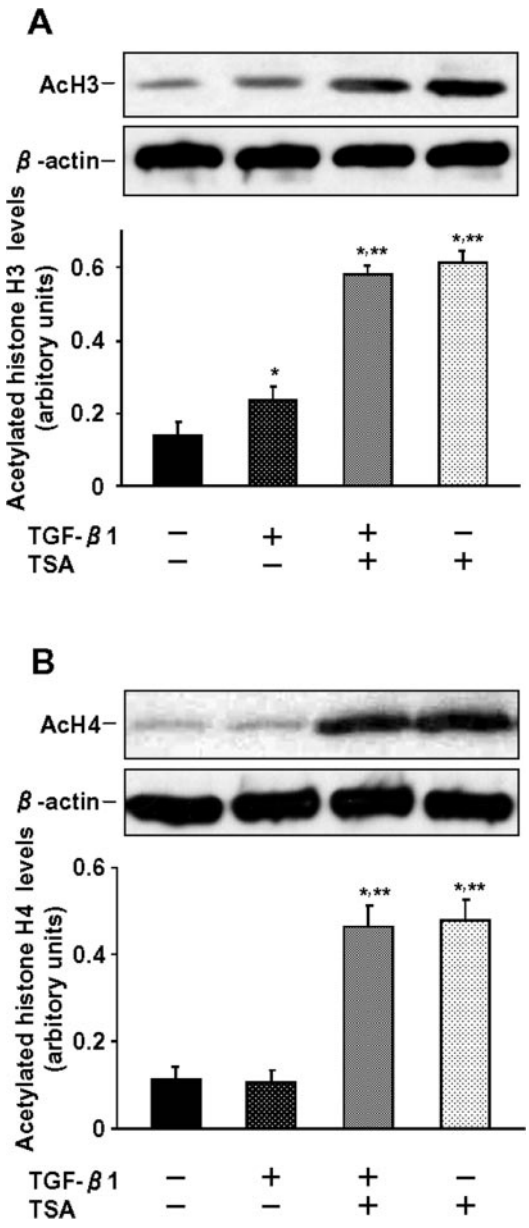

Figure 5. Acetylated histones H3 and H4 are increased by treatment with TSA. Whole lysates of RPTEC that were treated with TGF-β1 (3 ng/ml) and TSA (300 nM) for 6 h were Western-blotted with specific antibodies against acetylated histone H3 (AcH3) and H4 (AcH4). Representative Western immunoblot of AcH3 (A, top) and AcH4 (B, top) and their graphical presentation (A and B, bottom) are shown. Data are means ± SEM of seven independent experiments. *$P < 0.05$ *versus* control; **$P < 0.05$ *versus* TGF-β1–treated RPTEC.

Discussion

HDAC inhibitors prevent fibrosis in the liver (19), skin (15), and lung (20), but most of their underlying mechanisms remain to be elucidated. Although TSA improves renal disease in the MRL-lpr/lpr mouse (16), it is not known whether TSA prevents EMT in human renal epithelial cells. In this study, we demonstrated that TSA prevented TGF-β1–induced EMT in human

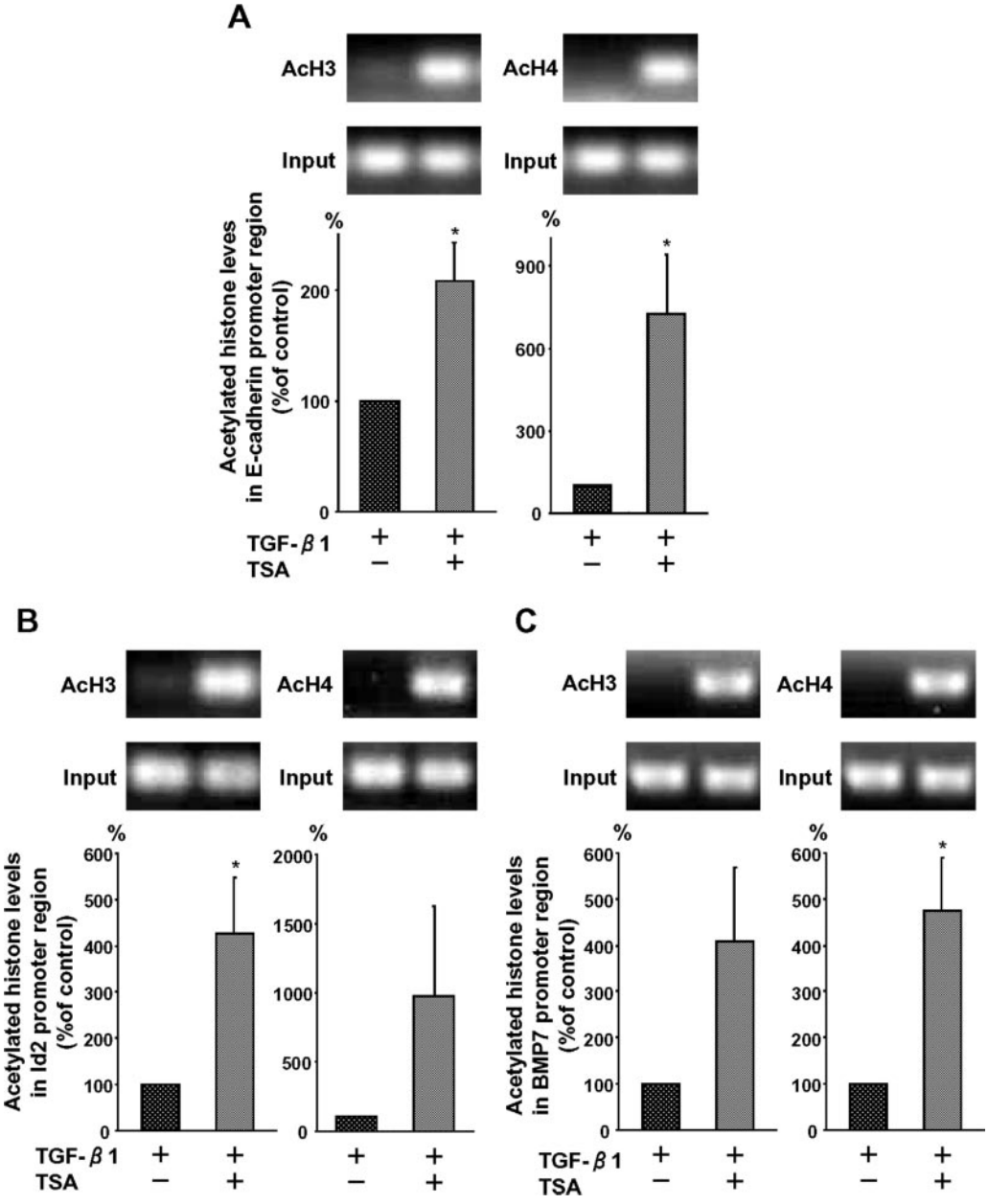

Figure 6. TSA-induced histone remodeling regulates some gene expression. Chromatin immunoprecipitation assay of the E-cadherin (A), Id2 (B), and BMP-7 (C) promoter regions in RPTEC that were treated with TGF-β1 (3 ng/ml) and TSA (300 nM) for 6 h. Immunoprecipitation was performed using specific antibodies against AcH3 (A through C, left) and AcH4 (A through C, right), and PCR was performed using specific primers for the E-cadherin (A), Id2 (B), and BMP-7 (C) promoter region. Representative PCR bands of the E-cadherin (A, top), Id2 (B, top), and BMP-7 (C, top) promoter region and their graphical presentation (A through C, bottom) are shown. Aliquots of samples before immunoprecipitation (Input) also were analyzed by PCR to quantify the amount of DNA present in different samples (A through C, top). Data are means ± SEM of four independent experiments. *$P < 0.05$ *versus* TGF-β1–treated RPTEC.

RPTEC and induced Id2 and BMP-7 that antagonize TGF-β1 signals.

TGF-β1 signals normally are transmitted to the nucleus through phosphorylation of R-Smads Smad2 and/or Smad3, which then form heterocomplexes with Smad4 (2,7). In our experiments, TGF-β1 induced phosphorylation of Smad2 and Smad3, which was not altered by co-treatment with TSA. This suggests that TSA is likely to suppress TGF-β1–induced tubular EMT downstream of R-Smad phosphorylation, and these results are compatible with the induction of Id2 and BMP-7 by co-treatment with TSA. It is reported that BMP-7 antagonizes TGF-β1–induced EMT in mouse distal tubular epithelial cells (3), inhibits TGF-β1–dependent profibrogenic activities in murine mesangial cells (1), and also prevents renal injury in a rat model of ureteral obstruction (30) in which TGF-β1 is a key molecule in the development of tubulointerstitial fibrosis (31).

Many factors inhibit BMP-7 signals, such as noggin and chordin, but no known factor or compound upregulates expression of BMP-7. Recently, Lin *et al.* (32) reported that kielin/chordin-like protein enhanced the BMP signal, but our results showed that TSA upregulated expression of BMP-7 itself.

Liu *et al.* (10) suggested that HGF antagonizes the profibrogenic action of TGF-β1 in mesangial cells and tubular epithelial cells by inducing Smad transcriptional co-repressors TGIF and SnoN, respectively. HGF also was reported to retard the progression of chronic obstructive nephropathy models (11), but its underlying mechanisms remain unknown (12). Recently, it was shown that expression of Id, which antagonizes basic helix-loop-helix transcription factors, was increased by BMP-7, and ectopic expression of Id2 and Id3 rendered epithelial cells refractory to TGF-β1–induced EMT (13). This suggests there are distinct basic helix-loop-helix factors that regulate the process of EMT and that are antagonized by Id2 and Id3, but these entities are not clear (13). Although TSA failed to upregulate HGF, TSA augmented gene expression of BMP-7 and Id2 even in the presence of TGF-β1. These results suggest that the inhibitory effects of TSA on TGF-β1–induced tubular EMT may be mediated through these factors. However, because gene expression of BMP-7 and Id2 increased by only two- to three-fold in the real-time reverse transcriptase–PCR, their definite roles still are unclear. To clarify these points, we examined the effect of small interference RNA (siRNA) for these factors. We used commercially available siRNA for BMP-7 and well-established siRNA for Id2 (13), but we could not get enough gene knockdown. Because human RPTEC is damaged easily and may not be good enough for siRNA studies, the definite role of these factors remains to be determined. Rombouts *et al.* (15) showed that TSA suppresses TGF-β1–induced fibrosis with an increase of TGIF, and our results showed that TSA upregulated Id2. However, we should be careful to speculate the effect of TSA *in vivo*. We examined the effect of TSA on a mouse model of ureteral obstruction (30) in which TGF-β1 is a key molecule in the development of tubulointerstitial fibrosis (31). Although there was some variation of fibrosis in this model, we confirmed that TSA inhibited progression of kidney fibrosis. However, we could not find significant effect of TSA on E-cadherin gene expression (unpublished data, M.Y., 2005). This discrepancy between *in vitro* and *in vivo* studies is probably because kidney fibrosis, *in vivo*, is not simply mediated by TGF-β1 alone, as in the *in vitro* model (33).

Next we investigated whether the changes in gene expression described previously were due to chromatin remodeling that was induced by TSA. Western blotting analysis showed an increase in total amounts of acetylated histones among the whole chromatin (Figure 5), but it is not clear which individual gene actually was regulated by the effect of TSA. Therefore, we performed ChIP assay for the E-cadherin, Id2, and BMP-7 genes, which were upregulated by treatment with TSA. The result indicated that expression of at least these three genes was increased through chromatin remodeling by TSA (Figure 6). Because BMP-7 is known to effect Id2 and E-cadherin expression, it may be possible that TSA induced BMP-7, which in turn increased Id2 expression and E-cadherin expression. Because it is reported that only <10% of gene expression is increased by the effect of HDAC inhibitors (16,34), comprehensive analysis such as microarray analysis will be required to determine all of the genes that are involved in prevention of TGF-β1–induced tubular EMT by TSA.

TSA and other HDAC inhibitors were reported to induce apoptosis in some cancer cells. In our experiments, the concentration of TSA was almost the same or even higher (up to 1 μM) than the concentration that induces apoptosis in cancer cells (17,18,35–37), but we could not find any toxicity in human RPTEC. Recently, it was reported that HDAC inhibitors induced tumor-selective toxicity through activation of the death receptor pathway (38). These results suggest that TSA can be used for the treatment of tubular EMT without overt toxicity.

Conclusion

Our results showed that inhibition of HDAC activity suppresses tubular EMT that is induced by TGF-β1. The precise mechanism remains to be determined, but our results showed that TSA induced several inhibitory factors of TGF-β1 signals, such as Id2 and BMP-7, in human RPTEC. These results suggest that TSA and other HDAC inhibitors could be new therapeutic agents for tubular EMT.

Disclosures

None.

References

1. Wang S, Hirschberg R: Bone morphogenetic protein-7 signals opposing transforming growth factor beta in mesangial cells. *J Biol Chem* 279: 23200–23206, 2004
2. Zeisberg M, Kalluri R: The role of epithelial-to-mesenchymal transition in renal fibrosis. *J Mol Med* 82: 175–181, 2004
3. Zeisberg M, Hanai J, Sugimoto H, Mammoto T, Charytan D, Strutz F, Kalluri R: BMP-7 counteracts TGF-beta1-induced epithelial-to-mesenchymal transition and reverses chronic renal injury. *Nat Med* 9: 964–968, 2003
4. Sato M, Muragaki Y, Saika S, Roberts AB, Ooshima A: Targeted disruption of TGF-beta1/Smad3 signaling protects against renal tubulointerstitial fibrosis induced by unilateral ureteral obstruction. *J Clin Invest* 112: 1486–1494, 2003
5. Dai C, Liu Y: Hepatocyte growth factor antagonizes the profibrotic action of TGF-beta1 in mesangial cells by stabilizing Smad transcriptional corepressor TGIF. *J Am Soc Nephrol* 15: 1402–1412, 2004
6. Prunier C, Howe PH: Disabled-2 (Dab2) is required for transforming growth factor beta-induced epithelial to mesenchymal transition (EMT). *J Biol Chem* 280: 17540–17548, 2005
7. Liu Y: Epithelial to mesenchymal transition in renal fibrogenesis: Pathologic significance, molecular mechanism, and therapeutic intervention. *J Am Soc Nephrol* 15: 1–12, 2004
8. Zhao J, Shi W, Wang YL, Chen H, Bringas P Jr, Datto MB, Frederick JP, Wang XF, Warburton D: Smad3 deficiency attenuates bleomycin-induced pulmonary fibrosis in mice. *Am J Physiol Lung Cell Mol Physiol* 282: L585–L593, 2002
9. Li Y, Yang J, Dai C, Wu C, Liu Y: Role for integrin-linked

kinase in mediating tubular epithelial to mesenchymal transition and renal interstitial fibrogenesis. *J Clin Invest* 112: 503–516, 2003
10. Liu Y: Hepatocyte growth factor in kidney fibrosis: Therapeutic potential and mechanisms of action. *Am J Physiol Renal Physiol* 287: F7–F16, 2004
11. Gao X, Mae H, Ayabe N, Takai T, Oshima K, Hattori M, Ueki T, Fujimoto J, Tanizawa T: Hepatocyte growth factor gene therapy retards the progression of chronic obstructive nephropathy. *Kidney Int* 62: 1238–1248, 2002
12. Yang J, Dai C, Liu Y: A novel mechanism by which hepatocyte growth factor blocks tubular epithelial to mesenchymal transition. *J Am Soc Nephrol* 16: 68–78, 2005
13. Kowanetz M, Valcourt U, Bergstrom R, Heldin CH, Moustakas A: Id2 and Id3 define the potency of cell proliferation and differentiation responses to transforming growth factor beta and bone morphogenetic protein. *Mol Cell Biol* 24: 4241–4254, 2004
14. Kondo M, Cubillo E, Tobiume K, Shirakihara T, Fukuda N, Suzuki H, Shimizu K, Takehara K, Cano A, Saitoh M, Miyazono K: A role for Id in the regulation of TGF-beta-induced epithelial-mesenchymal transdifferentiation. *Cell Death Differ* 11: 1092–1101, 2004
15. Rombouts K, Niki T, Greenwel P, Vandermonde A, Wielant A, Hellemans K, De Bleser P, Yoshida M, Schuppan D, Rojkind M, Geerts A: Trichostatin A, a histone deacetylase inhibitor, suppresses collagen synthesis and prevents TGF-beta(1)-induced fibrogenesis in skin fibroblasts. *Exp Cell Res* 278: 184–197, 2002
16. Mishra N, Reilly CM, Brown DR, Ruiz P, Gilkeson GS: Histone deacetylase inhibitors modulate renal disease in the MRL-lpr/lpr mouse. *J Clin Invest* 111: 539–552, 2003
17. Duan H, Heckman CA, Boxer LM: Histone deacetylase inhibitors down-regulate bcl-2 expression and induce apoptosis in t(14;18) lymphomas. *Mol Cell Biol* 25: 1608–1619, 2005
18. Henderson C, Mizzau M, Paroni G, Maestro R, Schneider C, Brancolini C: Role of caspases, Bid, and p53 in the apoptotic response triggered by histone deacetylase inhibitors trichostatin-A (TSA) and suberoylanilide hydroxamic acid (SAHA). *J Biol Chem* 278: 12579–12589, 2003
19. Niki T, Rombouts K, De Bleser P, De Smet K, Rogiers V, Schuppan D, Yoshida M, Gabbiani G, Geerts A: A histone deacetylase inhibitor, trichostatin A, suppresses myofibroblastic differentiation of rat hepatic stellate cells in primary culture. *Hepatology* 29: 858–867, 1999
20. Rishikof DC, Ricupero DA, Liu H, Goldstein RH: Phenylbutyrate decreases type I collagen production in human lung fibroblasts. *J Cell Biochem* 91: 740–748, 2004
21. Dai C, Yang J, Liu Y: Transforming growth factor-beta1 potentiates renal tubular epithelial cell death by a mechanism independent of Smad signaling. *J Biol Chem* 278: 12537–12545, 2003
22. Lofstedt T, Jogi A, Sigvardsson M, Gradin K, Poellinger L, Pahlman S, Axelson H: Induction of ID2 expression by hypoxia-inducible factor-1: A role in dedifferentiation of hypoxic neuroblastoma cells. *J Biol Chem* 279: 39223–39231, 2004
23. Ito K, Ito M, Elliott WM, Cosio B, Caramori G, Kon OM, Barczyk A, Hayashi S, Adcock IM, Hogg JC, Barnes PJ: Decreased histone deacetylase activity in chronic obstructive pulmonary disease. *N Engl J Med* 352: 1967–1976, 2005
24. Okada H, Danoff TM, Kalluri R, Neilson EG: Early role of Fsp1 in epithelial-mesenchymal transformation. *Am J Physiol* 273: F563–F574, 1997
25. Yang J, Liu Y: Blockage of tubular epithelial to myofibroblast transition by hepatocyte growth factor prevents renal interstitial fibrosis. *J Am Soc Nephrol* 13: 96–107, 2002
26. Bakin AV, Tomlinson AK, Bhowmick NA, Moses HL, Arteaga CL: Phosphatidylinositol 3-kinase function is required for transforming growth factor beta-mediated epithelial to mesenchymal transition and cell migration. *J Biol Chem* 275: 36803–36810, 2000
27. Janda E, Lehmann K, Killisch I, Jechlinger M, Herzig M, Downward J, Beug H, Grunert S: Ras and TGFbeta cooperatively regulate epithelial cell plasticity and metastasis: Dissection of Ras signaling pathways. *J Cell Biol* 156: 299–313, 2002
28. Manotham K, Tanaka T, Matsumoto M, Ohse T, Inagi R, Miyata T, Kurokawa K, Fujita T, Ingelfinger JR, Nangaku M: Transdifferentiation of cultured tubular cells induced by hypoxia. *Kidney Int* 65: 871–880, 2004
29. Yang J, Zhang X, Li Y, Liu Y: Downregulation of Smad transcriptional corepressors SnoN and Ski in the fibrotic kidney: An amplification mechanism for TGF-beta1 signaling. *J Am Soc Nephrol* 14: 3167–3177, 2003
30. Klahr S: The bone morphogenetic proteins (BMPs). Their role in renal fibrosis and renal function. *J Nephrol* 16: 179–185, 2003
31. Inazaki K, Kanamaru Y, Kojima Y, Sueyoshi N, Okumura K, Kaneko K, Yamashiro Y, Ogawa H, Nakao A: Smad3 deficiency attenuates renal fibrosis, inflammation, and apoptosis after unilateral ureteral obstruction. *Kidney Int* 66: 597–604, 2004
32. Lin J, Patel SR, Cheng X, Cho EA, Levitan I, Ullenbruch M, Phan SH, Park JM, Dressler GR: Kielin/chordin-like protein, a novel enhancer of BMP signaling, attenuates renal fibrotic disease. *Nat Med* 11: 387–393, 2005
33. Klahr S, Morrissey J: Obstructive nephropathy and renal fibrosis: The role of bone morphogenic protein-7 and hepatocyte growth factor. *Kidney Int Suppl* 87: S105–S112, 2003
34. De Felice L, Tatarelli C, Mascolo MG, Gregorj C, Agostini F, Fiorini R, Gelmetti V, Pascale S, Padula F, Petrucci MT, Arcese W, Nervi C: Histone deacetylase inhibitor valproic acid enhances the cytokine-induced expansion of human hematopoietic stem cells. *Cancer Res* 65: 1505–1513, 2005
35. Strait KA, Warnick CT, Ford CD, Dabbas B, Hammond EH, Ilstrup SJ: Histone deacetylase inhibitors induce G2-checkpoint arrest and apoptosis in cisplatinum-resistant ovarian cancer cells associated with overexpression of the Bcl-2-related protein Bad. *Mol Cancer Ther* 4: 603–611, 2005
36. Yee SB, Kim MS, Baek SJ, Kim GC, Yoo KS, Yoo YH, Park BS: Trichostatin A induces apoptosis of p815 mastocytoma cells in histone acetylation- and mitochondria-dependent fashion. *Int J Oncol* 25: 1431–1436, 2004
37. Fronsdal K, Saatcioglu F: Histone deacetylase inhibitors differentially mediate apoptosis in prostate cancer cells. *Prostate* 62: 299–306, 2005
38. Insinga A, Monestiroli S, Ronzoni S, Gelmetti V, Marchesi F, Viale A, Altucci L, Nervi C, Minucci S, Pelicci PG: Inhibitors of histone deacetylases induce tumor-selective apoptosis through activation of the death receptor pathway. *Nat Med* 11: 71–76, 2005